

Electron and ion imaging of gland cells using the FIB/SEM system

D. DROBNE, M. MILANI*, A. ZRIMEC†, V. LEŠER & M. BERDEN ZRIMEC†

Department of Biology, University of Ljubljana, Večna pot 111, SI–1000 Ljubljana, Slovenia

*Materials Science Department, University of Milano-Bicocca, Via Cozzi 53, I–20125 Milano, Italy

†Institute of Physical Biology, Velika Loka 90, SI–1290 Grosuplje, Slovenia

Key words. biological cell, digestive gland epithelium, FIB/ SEM system, *Porcellio scaber*, ultramicroscopy.

Summary

The FIB/SEM system was satisfactorily used for scanning ion (SIM) and scanning electron microscopy (SEM) of gland epithelial cells of a terrestrial isopod *Porcellio scaber* (Isopoda, Crustacea). The interior of cells was exposed by site-specific *in situ* focused ion beam (FIB) milling. Scanning ion (SI) imaging was an adequate substitution for scanning electron (SE) imaging when charging rendered SE imaging impossible. No significant differences in resolution between the SI and SE images were observed. The contrast on both the SI and SE images is a topographic. The consequences of SI imaging are, among others, introduction of Ga⁺ ions on/into the samples and destruction of the imaged surface. These two characteristics of SI imaging can be used advantageously. Introduction of Ga⁺ ions onto the specimen neutralizes the charge effect in the subsequent SE imaging. In addition, the destructive nature of SI imaging can be used as a tool for the gradual removal of the exposed layer of the imaged surface, uncovering the structures lying beneath. Alternative SEM and SIM in combination with site-specific *in situ* FIB sample sectioning made it possible to image the submicrometre structures of gland epithelium cells with reproducibility, repeatability and in the same range of magnifications as in transmission electron microscopy (TEM). At the present state of technology, ultrastructural elements imaged by the FIB/SEM system cannot be directly identified by comparison with TEM images.

Introduction

The application of focused ion beam (FIB) instruments is a rapidly growing research area (Inkson & Newcomb, 2004). It

is mainly related to microelectronics, with exciting uses of FIB technology in nanoscale research (Perrey *et al.*, 2004). The FIB is widely employed in site-specific 2D sectioning and imaging of microstructures (Phaneuf, 1999; Inkson *et al.*, 2001; Steer *et al.*, 2002; Sivel *et al.*, 2004). The combination of *in situ* FIB sectioning with scanning ion (SI) and/or scanning electron (SE) imaging has attracted significant attention.

The FIB/SEM system is a combination of a FIB and an electron beam and secondary ion and secondary electron detectors. FIB gallium (Ga⁺) ions operated at low beam currents are used for imaging, and high beam currents are used for site-specific sputtering or milling. As the Ga⁺ primary ion beam rasters on the sample surface, the signal from the sputtered (secondary) ions or secondary electrons is collected to form an image (Goodhew *et al.*, 2001). The imaging resolution of FIB improved in the latter half of 1990s to the level where FIB instruments can compete with conventional scanning electron microscopes (SEMs) (Phaneuf, 1999).

In SE images, a topographic contrast is prevalent. This contrast mechanism is explained in terms of differences in signal, which is a function of the angle of incidence of the primary beam relative to the specimen surface as the local inclination of the specimen surface varies. To extract the maximum information from the investigated specimen, low voltage SEM (LV-SEM) instruments may also be operated, where the primary energy may be as low as 0.2 keV and where beside lateral detector Everhart-Thorney type, ET, different in-lens and out-lens detection system are used (Cazaux, 2004). In scanning ion microscopy (SIM) of material science specimens, contrast mechanisms are also related to the crystallographic orientation (channelling) contrast and material contrast. Several contrast mechanisms interact simultaneously in typical SI images and, as in most beam instruments, suppressing or enhancing one particular mechanism can enhance details in the image (Phaneuf, 1999; Sakai *et al.*, 1999; Ohya & Ishitani, 2002,

Correspondence to: Tel: +386 1 4233388; fax: +386 1 2573390; e-mail: damjana.drobne@bf.uni-lj.si

2003a). In SIM of biological samples of an irregular shape, the topographic contrast is expected to prevail as it does in SEM.

A promising advantage of FIB microscopy over conventional SEM is that charging of a sample is not a problem. The specimen becomes electrically charged when it starts to receive more electrons than it is emitting, or vice versa. The presence of charge generates an electric field that may interfere with the collection of secondary electrons, deflect the incident beam or even damage the specimen (Joy & Joy, 1996). In developing modern field emission gun (FEG) microscopes, much of the interest was motivated by the hope that charging would be eliminated by the use of lower incident energies (LV-SEM). However, in poorly conductive or insulating uncoated specimens, charging remains a problem. Coating of samples with heavy metals or carbon reduces charging of a sample, but even the thinnest film obscures the surface to some degree (Joy & Joy, 1996; Goodhew *et al.*, 2001). Recently, variable pressure scanning electron microscopes (VP-SEM) have been developed, where gas (laboratory air or water vapour) is introduced into the chamber which neutralizes the charge at the sample surface, but the presence of gas in the chamber prevents the use of conventional secondary electron detectors (Robertson *et al.*, 2005).

In the life sciences, applications of SIM for structure analysis are scarce (Ballerini *et al.*, 1997; Drobne *et al.*, 2004; Milani *et al.*, 2004). Ion imaging of biological material is related to mass spectrometry providing images of elements and organic substances (Mony & Larras-Regard, 1997; Almqvist *et al.*, 2001; Chandra, 2003; Okabe *et al.*, 2003; Takaya *et al.*, 2003, 2004).

The aim of our work was to apply the FIB/SEM system to the imaging of cellular structures. We conducted SIM and SEM on gland epithelial cells of a terrestrial isopod *Porcellio scaber* (Isopoda, Crustacea) that has been investigated by a variety of microscopy techniques (Žnidaršič *et al.*, 2003; Drobne *et al.*, 2004, 2005). Improvements in using alternative SE and SI imaging, together with *in situ* FIB milling in structural investigations of a cell, are discussed.

Materials and methods

Terrestrial isopods, *Porcellio scaber* (Latreille, 1809) (Isopoda, Crustacea), were collected under concrete blocks and pieces of decaying wood. For histological observation, digestive glands were fixed in Carnoy-B fixative for 2.5 h at room temperature, dehydrated in ethanol series and embedded in paraplast. 8 µm sections were stained with eosin. For SEM and SIM operations digestive gland tubes were isolated and fixed in 1.0% glutaraldehyde and 0.4% paraformaldehyde in 0.1 M sodium cacodylate buffer (pH 7.2) for 2.5 h at room temperature. The postfixation of samples was omitted in order to wash out the large amounts of lipids that fill the digestive gland cells. In this way we gained empty volumes. No other deep-etching chemical procedures were performed (Martinez & DeSouza, 1997). After dehydration in a graded series of ethanols, the digestive

Table 1. Ion milling, cleaning milling, ion and electron imaging parameters used in the study.

	Ion milling	Cleaning milling	SIM	SEM
Ion currents	5–7 nA	300 pA–1 nA	10–350 pA	–
Beam energy (keV Ga ⁺)	30	30	30	–
Beam diameter (nm)	200–300	50–100	15	5
Overlap (%)	50	50	50	50

gland tubes were dried at the critical point (Balzers Critical Point Dryer 030, Liechtenstein) and gold sputtered (sputter coater SCD 050, BAL-TEC, Germany).

The dried samples were mounted on brass holders with silver paint (high purity silver paint, SPI), fixed on a standard holder (6 cm diameter, 5-axis eucentric stage) and placed into a Dual Beam system for FIB/SEM operation (FEI Strata DB 235 M). Gallium ions were field emitted from a liquid metal ion source (Table 1).

SEM imaging was performed by means of the FEG electron column available in the same system (Table 1). The system operated with column pressures in the 10⁻⁵ Pa range with the work chamber between 10⁻⁴ and 10⁻³ Pa.

All together, seven animals were investigated and the FIB/SEM operation was conducted on nine successive occasions. Operations are highly reproducible and the results repeatable. In this paper we present the SE and SI imaging of two of these animals.

Results

The light micrograph (Fig. 1) shows a histological image of a cross section of a digestive gland tube that is composed of a single layer epithelium. We interpret the numerous empty round shaped regions of different sizes as areas inside the cells where lipid droplets were originally deposited.

FIB milling was conducted on mechanically broken gland tubes (Fig. 2a,b). The outside of the tubes was gold coated, the inside was uncoated. Here, the charging effect is evident. It appears either as evidently brighter areas in comparison to the rest (Fig. 2a), bright areas free of structures (Fig. 2b) or as a degraded image (Fig. 5a).

The shape and dimensions of the FIB cut are shown on an ion image taken after the milling operation (Fig. 3). The exposed cell surface was then SE and SI imaged (Figs 4a,b, 5a,b,c, 6a,b). The charging effect was also pronounced on the uncoated FIB milled region of a cell (Figs 4a, 5a), but this is not a problem for SIM (Figs 4b, 6a). The charging rendered SE imaging impossible at moderate magnifications of irregularly shaped structures. In such cases the problem of imaging was satisfactory solved by using SI imaging (Figs 4b, 6a). The charging effect was lower where the imaged region was flatter and with increasing magnification (Figs 2b, 5a,b,c). Note the very high

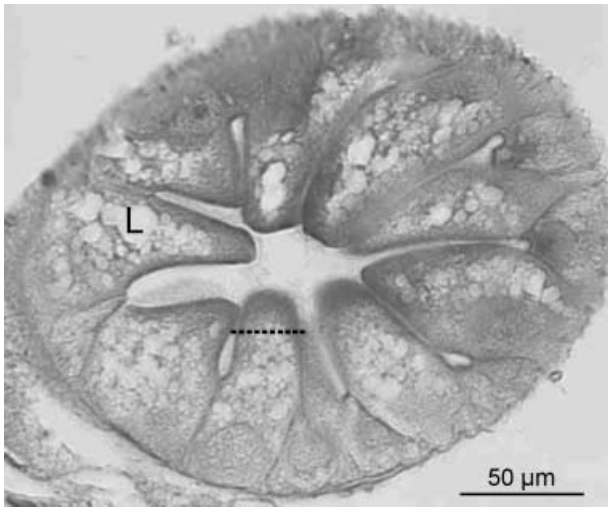


Fig. 1. Light micrograph of cross section of a digestive gland tube. L, region where a lipid droplet was deposited. The dotted line indicates the approximate position of a FIB cut.

magnification (250 kX) with no charge effect and good resolution on the SE image (Fig. 5c). The contrast on the SE images is different to that on the SI ones, but the quality of the images is similar (Figs 4a,b, 5a,b, 6a). SI imaged cell surfaces have a characteristic 'tin plating' appearance (Figs 4b, 6a, 7a).

Alternate SE/SI/SE imaging was performed on another FIB milled cell (Figs 6b, 7a,b). After SE imaging, three successive ion imaging operations were performed with different ion currents: 350 pA, 120 pA (images not shown) and 33 pA (Fig. 7a). The final ion imaging (Fig. 7a) was followed by electron imaging (Fig. 7b). Note the reduced charging effect on Fig. 7(b) in comparison to Fig. 6(b) where the same area was electron imaged. A consequence of destructive ion beam imaging is seen as slightly different structural compositions of the investigated surface before and after SI imaging (compare Figs 6b and 7b). Mechanically less resistant structures are removed (Fig. 7b) and enlarged and multiplied holes in the walls of empty spheres can be seen.

Discussion

In previous work we used the FIB/SEM system for SI imaging of gross morphology of an organ system (Drobne *et al.*, 2004). It is difficult to distinguish between the SI and SE images obtained for the digestive system (Drobne *et al.*, 2004). In the present study, we focused on imaging the ultrastructure of cells by a FIB/SEM system. The interior of cells was exposed by *in situ* FIB milling. The milling parameters and the milling artefacts on the same type of epithelium are described elsewhere (Drobne *et al.*, 2005).

No significant differences in resolution between the SI and SE images of FIB milled digestive gland epithelium cell were

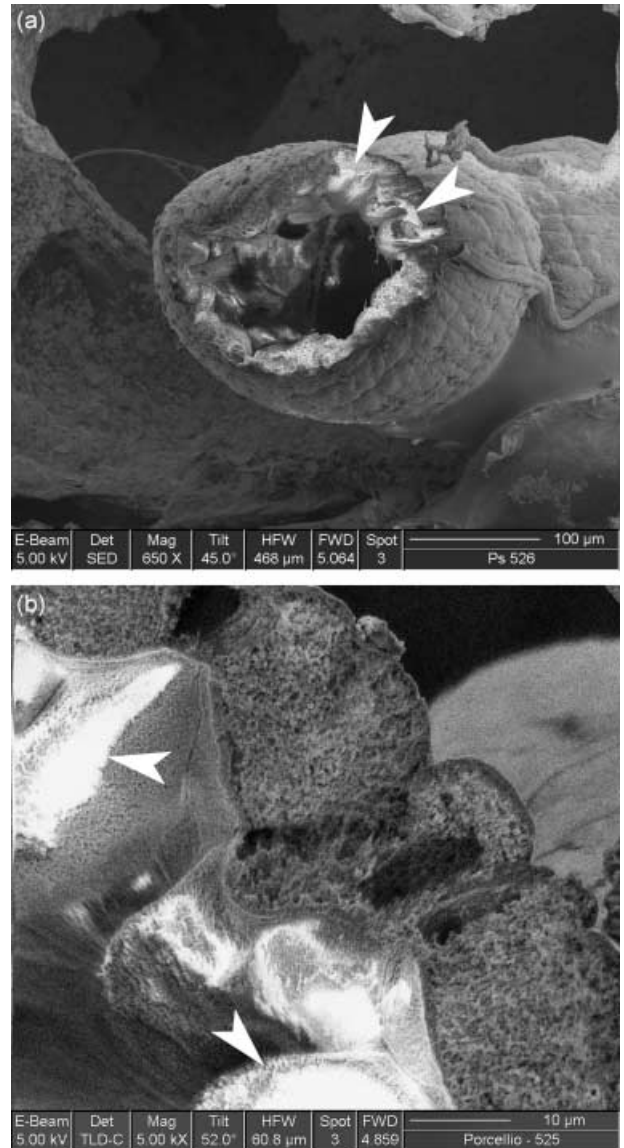


Fig. 2. Scanning electron micrograph of a mechanically broken digestive gland tube (a) and part of the digestive gland tube where the FIB operation was performed (b). Arrowheads indicate regions where intensive charging of the sample is present.

observed, although the images are different. The higher penetration of the electron beam into the sample leads to enhanced SE emission producing the characteristic 3D appearance associated with SEM images (Joy & Joy, 1996). Due to lower penetration of ions into the surface during SI imaging, the signal originates from the top layer of the specimen and the imaged region has a characteristic 'tin plating' appearance.

The contrast, on both SI and SE images is topographic (Ohya & Ishitani, 2003b; Milani *et al.*, 2004). In some regions there are pronounced differences in contrast between the two images (compare Fig. 4a and b). Holes in specimens observed

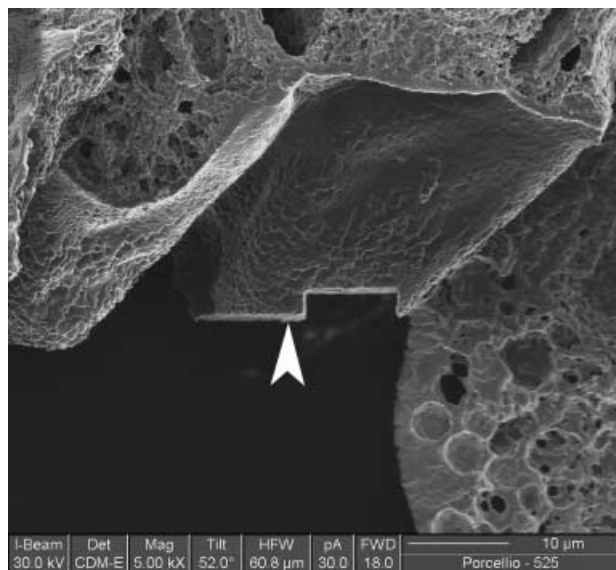


Fig. 3. Scanning ion micrograph of the position and dimensions of the FIB cut.

using SE are brighter than the surroundings because of the charging effect. On SI images these structures are darker because they emit less signal compared to the rest of the imaged area. As expected, the heterogeneous nature of the chemical composition of a biological sample was not recognized by SI imaging.

Among others, the consequences of SI imaging are: introduction of the Ga^+ ions on/into the samples and destruction of the imaged surface. Both of these characteristics of SIM can be used advantageously. Introduction of positive Ga ions into the samples reduces the charge effect. A shower of positive ions has a similar effect as gas in VP-SEM; both neutralize the charge at the sample surface (Robertson *et al.*, 2005). In addition, the destructive nature of SI imaging can be used as a tool for the gradual removal of the exposed layer of the imaged surface, uncovering the underlying structures.

Imaging of irregular 3D biological structures at the sub-micrometre scale is mostly confined to transmission electron microscopy (TEM) (Afzelius & Maunsbach, 2004; McIntosh *et al.*, 2005). Some amazing data and pictures have also been obtained from Field-Emission SEM (FESEM) and cryo-SEM (Erlandsen *et al.*, 2000; Walther, 2003). Atomic force microscopy (AFM) and scanning tunnel microscopy (STM) have also been used for ultrastructural research of biological samples down to the nanometre level, but their limitation is a small volume coverage from which good quality images can be obtained (Permjakov *et al.*, 1999; Mariani *et al.*, 2001; Alonso & Goldmann, 2003; Grant & McDonnell, 2003).

SEM is not the usual method of choice for cellular ultrastructure research. First of all, samples for conventional SEM are not prepared with an exposed interior, and secondly, sooner or later, the charging effect dissuades potential users

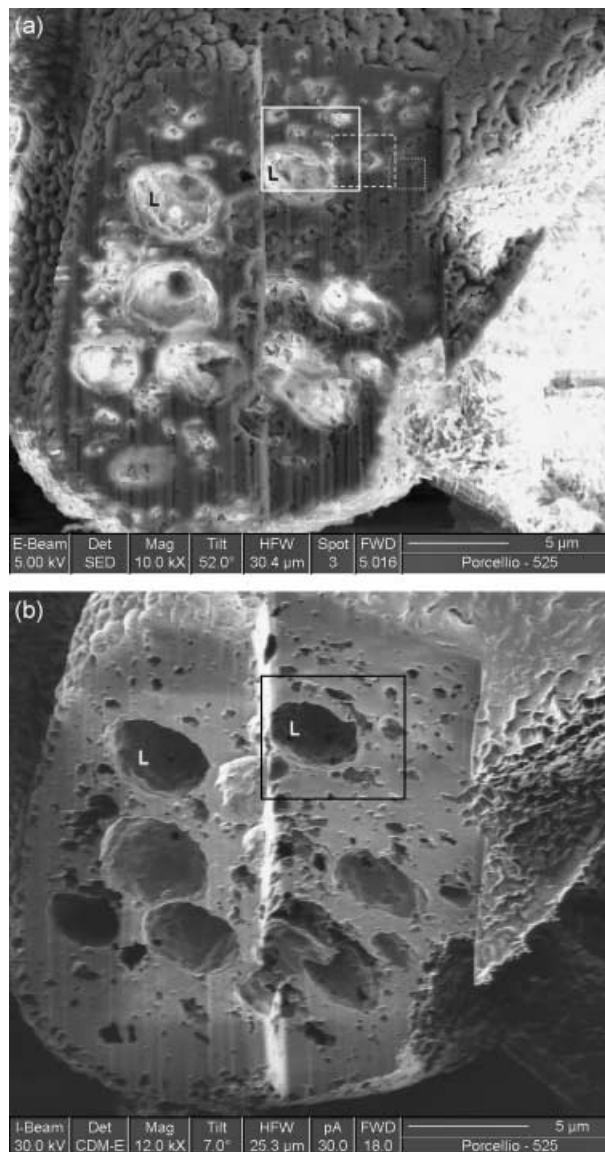


Fig. 4. (a) Scanning electron micrograph of a FIB milled cell. Regions marked with the solid, dashed and dotted lines are magnified and shown in Fig. 5(a–c). (b) Scanning ion micrograph of the same cell. The region marked with the square is magnified and shown in Fig. 6(a). L, regions where lipids were deposited.

from the application of SEM for ultrastructure research in the life sciences. In our work, the problem with site specific 'entering' into the imaged cells was solved by *in situ* FIB milling and the problem with sample charging was kept under control by a combination of SE and SI imaging modes. We succeeded in imaging the ultrastructure of gland cells with reproducibility, repeatability and in the same range of magnifications as TEM. At the current state of technology, the ultrastructural elements imaged by the FIB/SEM system cannot be directly identified by comparison with TEM images (Žnidaršič *et al.*, 2003). Substantial work is needed before the identification

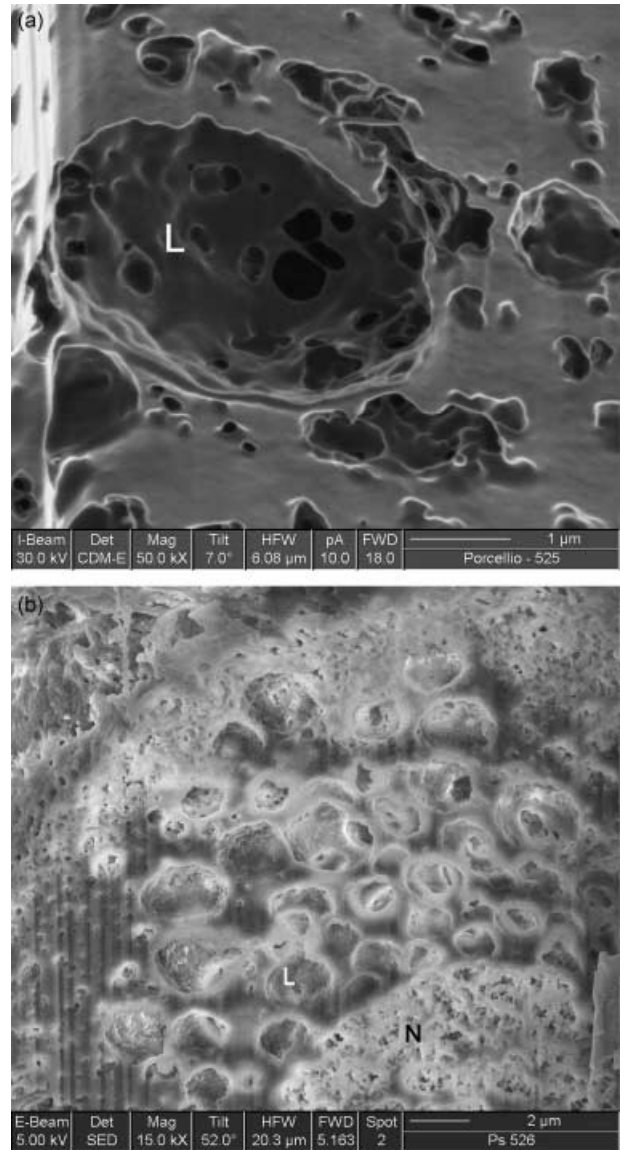
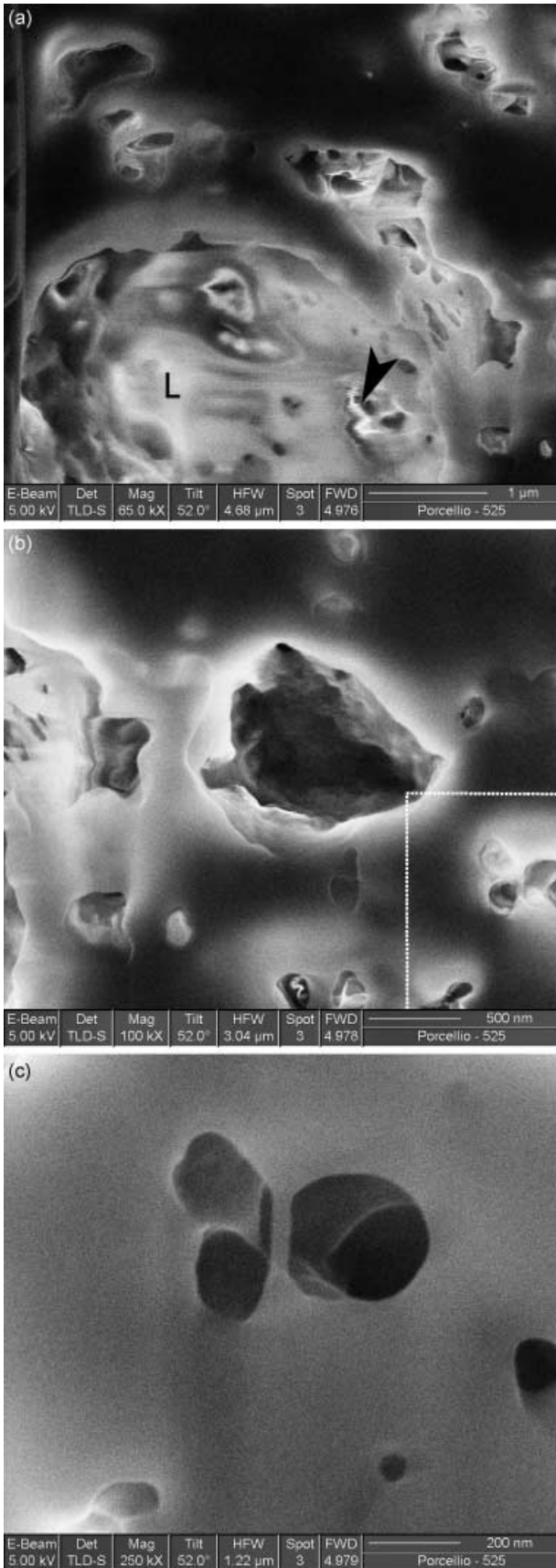


Fig. 6. (a) Scanning ion micrograph of a region marked on Fig. 4(b). (b) Scanning electron micrograph of a middle part of a FIB milled cell. The exposed surface was subsequently SI imaged. L, region where a lipid droplet was deposited; N, nucleus.

of ultrastructural elements of cells imaged by the FIB/SEM system is possible.

The possibility of extracting the electron signal by scanning the same region of a biological sample using electrons or ions is a novelty. There are no limitations to upgrading the FIB/SEM system by installing even more detectors inside the chamber (energy-dispersive X-ray detectors, ion detectors, elements of scanning probe microscopes, etc.). Such an instrument would

Fig. 5. Scanning electron micrographs of regions marked on Fig. 4(a). L, region where a lipid droplet was deposited. Arrowhead indicates image degradation due to microdischarges.

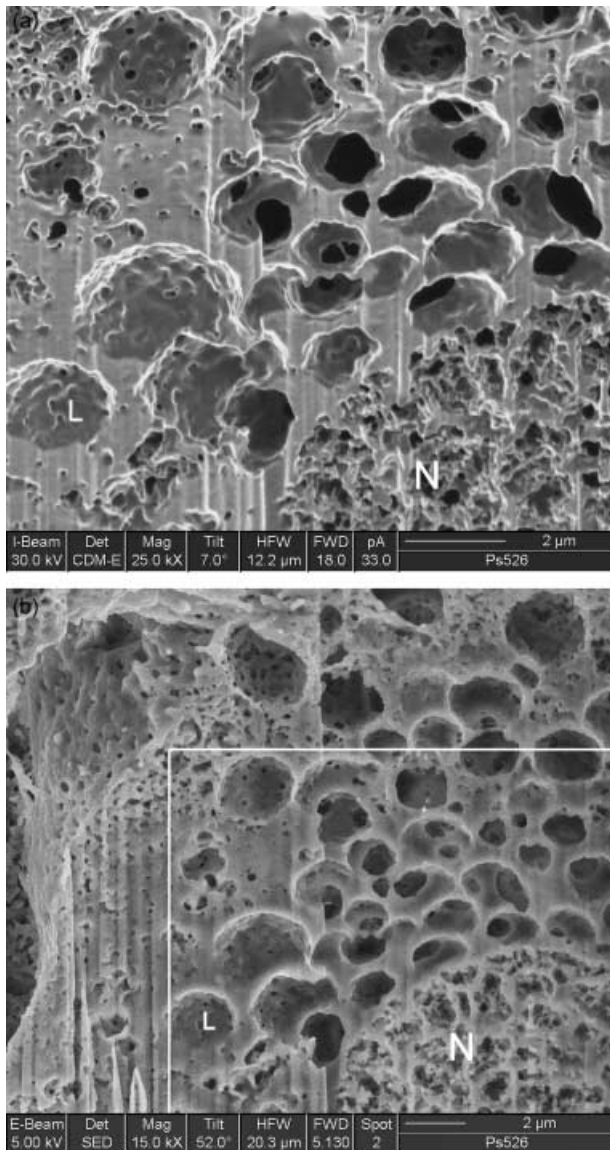


Fig. 7. (a) Scanning ion micrograph of a similar region to that shown in Fig. 6(b). (b) Scanning electron micrograph of the same region as in Fig. 7(a) after three SIM operations. L, region where a lipid droplet was deposited; N, nucleus.

then offer many possibilities for imaging and elemental analyses in biomedicine (Permjakov *et al.*, 1999; Goodhew *et al.*, 2001; Alonso & Goldmann, 2003; Chandra, 2003; Yamamoto *et al.*, 2003; Xu *et al.*, 2004).

In conclusion, the FIB/SEM system enables site specific *in situ* FIB milling and SI and/or SE imaging of unstained, coated or uncoated nonconductive biological samples of an irregular shape down to the submicrometre level and provides more comprehensive microscopy results than any conventional microscopy technique in biomedicine. In spite of the evident potential applicability of the FIB/SEM system in the life sciences, it is not widely appreciated due to the lack of data for biological

samples that would allow possible users to make a critical evaluation of the technique.

Acknowledgements

We thank Francesco Tatti from FEI Italy for his technical assistance with the FIB/SEM system and Kazimir Drašlar from the Department of Biology at the University of Ljubljana, Slovenia, for his help with sample preparation.

References

- Afzelius, B.A. & Maunsbach, A.B. (2004) Biological ultrastructure research; the first 50 years. *Tissue Cell*, **36**, 83–94.
- Almqvist, N., Delamo, Y., Smith, B.L., Thomson, N.H., Bartholdson, Å., Lal, R., Brzezinski, M. & Hansma, P.K. (2001) Micromechanical and structural properties of a pennate diatom investigated by atomic force microscopy. *J. Microsc.* **202**, 518–532.
- Alonso, J.L. & Goldmann, W.H. (2003) Feeling the forces: atomic force microscopy in cell biology. *Life Sci.* **72**, 2553–2560.
- Ballerini, M., Milani, M., Costato, M., Squadrini, F. & Turcu, I.C.E. (1997) Life science applications of Focused Ion Beams (FIB). *Eur. J. Histochem.* **41**, 89–90.
- Cazaux, J. (2004) About the role of the various types of secondary electrons (SE1; SE2; SE3) on the performance of LVSEM. *J. Microsc.* **214**, 341–347.
- Chandra, S. (2003) SIMS ion microscopy as a novel, practical tool for subcellular chemical imaging in cancer research. *Appl. Surf. Sci.* **203**, 679–683.
- Drobne, D., Milani, M., Ballerini, M., Zrimec, A., Berden Zrimec, M., Tatti, F. & Drašlar, K. (2004) Focused ion beam (FIB) for microscopy and for *in situ* sample preparation: application on a crustacean digestive system (*Porcellio scaber*, Isopoda, Crustacea). *J. Biomed. Opt.* **9**, 1238–1243.
- Drobne, D., Milani, M., Zrimec, A., Berden Zrimec, M., Tatti, F. & Drašlar, K. (2005) Focused ion beam/scanning electron microscopy studies of *Porcellio scaber* (Isopoda, Crustacea) digestive gland epithelium cells. *Scanning*, **27**, 30–34.
- Erlandsen, S.L., Frethem, C. & Chen, Y. (2000) Field emission scanning electron microscopy (FESEM) entering the 21st century: Nanometer resolution and molecular topography of cell structure. *J. Histotechnol.* **23**, 249–259.
- Goodhew, P.J., Humphreys, J. & Beanland, R. (2001) *Electron Microscopy and Analyses*. Taylor and Francis, London.
- Grant, A. & McDonnell, L. (2003) A non-contact mode scanning force microscope optimised to image biological samples in liquid. *Ultramicroscopy*, **97**, 177–184.
- Inkson, B.J. & Newcomb, S. (2004) Editorial. *J. Microsc.* **214**, 207.
- Inkson, B.J., Steer, T., Mobus, G. & Wagner, T. (2001) Subsurface nanoindentation deformation of Cu-Al multilayers mapped in 3D by focused ion beam microscopy. *J. Microsc.* **201**, 256–269.
- Joy, D.C. & Joy, C.S. (1996) Low voltage scanning electron microscopy. *Micron*, **27**, 247–263.
- Mariani, T., Ascoli, C., Baschieri, P., Frediani, C. & Musio, A. (2001) Scanning force images through the 'Milliscope' – a probe microscope with very wide scan range. *J. Microsc.* **204**, 53–60.
- Martinez, A.M.B. & DeSouza, W. (1997) A freeze-fracture and deep-etch study of the cuticle and hypodermis of infective larvae of *Strongyloides venezuelensis* (Nematoda). *Int. J. Parasitol.* **27**, 289–297.

- McIntosh, R., Nicastro, D. & Mastrorade, D. (2005) New views of cells in 3D: an introduction to electron tomography. *Trends Cell Biol.* **15**, 43–51.
- Milani, M., Ballerini, M., Batani, D., Squadrini, F., Cotelli, F., Donin, C.L.L., Polleti, G., Pozzi, A., Eidmann, K., Stead, A. & Lucchini, G. (2004) High resolution microscopy techniques for the analysis of biological samples: a comparison. *Eur. Phys. J.-Appl. Phys.* **26**, 123–131.
- Mony, M.C. & Larras-Regard, E. (1997) Imaging of subcellular structures by scanning ion microscopy and mass spectrometry. Advantage of cryo-fixation and freeze substitution procedure over chemical preparation. *Biol. Cell*, **89**, 199–210.
- Ohya, K. & Ishitani, T. (2002) Target material dependence of secondary electron images induced by focused ion beams. *Surf. Coat. Techn.* **158**, 8–13.
- Ohya, K. & Ishitani, T. (2003a) Comparative study of depth and lateral distributions of electron excitation between scanning ion and scanning electron microscopes. *J. Electron. Microsc.* **52**, 291–298.
- Ohya, K. & Ishitani, T. (2003b) Simulation study of secondary electron images in scanning ion microscopy. *Nucl. Instrum. Meth. B*, **202**, 305–311.
- Okabe, M., Yoshida, T., Yoshii, R., Sawataishi, M. & Takaya, K. (2003) Zinc detection in the islet of Langerhans by SIMS. *Appl. Surf. Sci.* **203**, 714–717.
- Permjakov, N.K., Ananyan, M.A., Luskinovich, P.N., Sorokovoi, V.I. & Saveliev, S.V. (1999) Use of STM for analysis of surfaces of biological samples. *Appl. Surf. Sci.* **145**, 146–150.
- Perrey, C.R., Carter, C.B., Michael, J.R., Kotula, P.G., Stach, E.A. & Radmilovic, V.R. (2004) Using the FIB to characterize nanoparticle materials. *J. Microsc.* **214**, 222–236.
- Phaneuf, M.W. (1999) Applications of focused ion beam microscopy to materials science specimens. *Micron*, **30**, 277–288.
- Robertson, K., Gauvin, R. & Finch, J. (2005) Application of charge contrast imaging in mineral characterization. *Miner. Eng.* **18**, 343–352.
- Sakai, Y., Yamada, T., Suzuki, T. & Ichinokawa, T. (1999) Contrast mechanisms of secondary electron images in scanning electron and ion microscopy. *Appl. Surf. Sci.* **145**, 96–100.
- Sivel, V.G.M., Van den Brand, J., Wang, W.R., Mohdadi, H., Tichelaar, F.D., Alkemade, P.F.A. & Zandbergen, H.W. (2004) Application of the dual-beam FIB/SEM to metals research. *J. Microsc.* **214**, 237–245.
- Steer, T.J., Mobus, G., Kraft, O., Wagner, T. & Inkson, B.J. (2002) 3-D focused ion beam mapping of nanoindentation zones in a Cu-Ti multilayered coating. *Thin Solid Films*, **413**, 147–154.
- Takaya, K., Okabe, M., Sawataishi, M., Takashima, H. & Yoshida, T. (2003) Fine structures and ion images on fresh frozen dried ultrathin sections by transmission electron and scanning ion microscopy. *Appl. Surf. Sci.* **203**, 684–688.
- Takaya, K., Okabe, M., Sawataishi, M. & Yoshida, T. (2004) Influence of hydrocarbons on element detection in ion images by SIMS microscopy. *Appl. Surf. Sci.* **231–2**, 502–505.
- Walthers, P. (2003) Recent progress in freeze-fracturing of high-pressure frozen samples. *J. Microsc.* **212**, 34–43.
- Xu, J., Ostrowski, S., Szakal, C., Ewing, A.G. & Winograd, N. (2004) ToF-SIMS imaging with cluster ion beams. *Appl. Surf. Sci.* **231–2**, 159–163.
- Yamamoto, D., Tani, K., Gotoh, T. & Kouyama, T. (2003) Direct observations of freeze-etching processes of ice-embedded biomembranes by atomic force microscopy. *Micron*, **34**, 9–18.
- Žnidaršič, N., Štrus, J. & Drobne, D. (2003) Ultrastructural alterations of the hepatopancreas in *Porcellio scaber* under stress. *Environ. Toxicol. Phar.* **13**, 161–174.